JOURNAL OF SOLID STATE CHEMISTRY 25, 179–187 (1978)

Phases in the $Ba_3Fe_{1+x}S_5$ Series: The Structure of β-$Ba_9Fe_4S_{15}$ and its Low-Temperature α Polymorph

S. COHEN, L. E. RENDON-DIAZMIRON, AND H. STEINFINK

Materials Science and Engineering, Department of Chemical Engineering, The University of Texas at Austin, Austin, Texas 78712

Received October 8, 1977; in revised form, December 23, 1977

The crystal structure of β-$Ba_9Fe_4S_{15}$ shows that it is a phase in the infinitely adaptive series of compounds $Ba_3Fe_{1+x}S_5$, $0 \leqslant x \leqslant 1$. The material is synthesized by reacting a slightly sulfur-rich mixture at 900°C in a sealed quartz ampoule. Lattice constants are $a = 25.212(3)$ Å, $b = 9.594(1)$ Å, $c = 12.575(1)$ Å, *Pnma*, $z = 4$. Three thousand thirty-three structure amplitudes were refined to $R = 0.049$. BaS_6 trigonal prisms share triangular faces to form infinite columns; the columns in turn share edges and create nearly hexagonal enclosures. Within these rings are additional Ba and S and tetrahedral interstices are created which can be occupied by Fe. The variation of the Fe occupancy from ring to ring gives rise to phases in which one dimension is an integral multiple of the 8.5-Å repeat observed in one end member of the series, Ba_3FeS_5. The other end member is $Ba_3Fe_2S_5$. At temperatures below 900°C a polymorphic phase is formed. Its lattice constants are $a = b = 9.634(1)$ Å, $c = 34.311(3)$ Å, $I4_1/a$, $z = 4$. One thousand five hundred eighty-three structure amplitudes were refined to $R = 0.0483$. Trigonal prisms and bisdisphenoids articulate to form a complex three-dimensional structure. Two of the S atoms in the structure have statistical site occupancies.

Introduction

Recently the crystal structures of two compounds, Ba_3FeS_5 and $Ba_{15}Fe_7S_{25}$, have been reported (*1*). The structures are closely related, the differences being due essentially to the filling by iron atoms of tetrahedral sites which exist within pseudohexagonal rings formed by edge sharing of BaS_6 trigonal prisms. Furthermore, the filling of the tetrahedral sites need not be identical from ring to ring, so that one can postulate the existence of an infinite number of compounds. The periodicity of one ring configuration is about 8.5 Å and as the sequences of tetrahedral occupancies within the rings are varied the periodicity along this axis becomes an integral multiple of 8.5 Å. To test the hypothesis that a series with the general formula $Ba_3Fe_{1+x}S_5$ exists, we attempted to prepare an additional compound in this series, $Ba_9Fe_4S_{15}$, in which one unit cell dimension should be triple that of the corresponding dimension in Ba_3FeS_5. In the process of preparing this phase another compound was discovered, which eventually turned out to have the same composition. The chemistry of these two phases is closely related and we report here their structures.

Experimental

The first attempts to prepare the expected phase, $Ba_9Fe_4S_{15}$, were undertaken by sealing the stoichiometric amounts of BaS–Fe–S into closed graphite ampoules which in turn were sealed in evacuated Vycor tubes. Several mixtures were reacted at about 1000°C for 3 days and at the end of the reaction time either air quenched or slowly cooled to room temperature. Very well-crystallized material

0022-4596/78/0252-0179$02.00/0

whose powder pattern identified it as $Ba_{15}Fe_7S_{25}$ was formed under these conditions. During the course of our studies we have observed that a slight excess of sulfur vapor pressure during the reaction frequently promotes the formation of a given composition and, therefore, we reacted a mixture in the proportion 9BaS:4Fe:8S under the previously described conditions. A product obtained at 900°C yielded a powder pattern which was very similar to that of $Ba_{15}Fe_7S_{25}$; the "*d*" values were nearly the same but the intensities of several lines varied significantly to indicate that, indeed, this might be the new phase.

Mixtures having this composition were now reacted between temperatures of 750 to 960°C in 50° intervals. The products were the same whether quenching in water or slowly cooling by shutting off power to the furnace. The powder pattern of the product obtained at the lowest temperature showed the presence of BaS, BaS_2, and a new phase. Above 900°C mixtures of $Ba_9Fe_4S_{15}$ and $Ba_{15}Fe_7S_{25}$ were observed. At about 850°C the X-ray diffraction powder pattern indicated that the primary constituent was a second new phase, later identified as having the same composition as the first. We designate the low-temperature phase as α and the high-temperature phase as β.

The Mössbauer spectra were obtained with equipment and under conditions previously described (*1*).

β-$Ba_9Fe_4S_{15}$

A black single crystal measuring 0.22 × 0.22 × 0.16 mm was selected from the 9BaS:4Fe:8S mixture reacted at 900°C. Preliminary Weissenberg and Buerger photographs showed diffraction symmetry *mmm* with the systematic absences $0kl$, $k + l = 2n + 1$ and $hk0$, $h = 2n + 1$, consistent with space groups *Pnma* and $Pna2_1$. Lattice constants were determined from a least-squares refinement of precise 2θ measurements of 41 reflections between 20 and 50°, using a quarter circle diffractometer and Mo radiation, λ_1 = 0.70926 Å (*1*). The crystal data obtained at room temperature are shown in Table I.

TABLE I

CRYSTALLOGRAPHIC DATA

	β-$Ba_9Fe_4S_{15}$	α-$Ba_9Fe_4S_{15}$
a (Å)	25.212(3)	9.634(1)
b	9.594(1)	9.634(1)
c	12.575(1)	34.311(3)
Space group	*Pnma*	$I4_1/a$
z	4	4
ρ_{calc} (g/cm³)	4.24	4.18
No. of F (hkl)	3033	1583
R	0.049	0.0483
wR	0.051	0.0510

Intensity data were collected to $\sin\theta/\lambda = 0.65$, on a Syntex $P2_1$ autodiffractometer using graphite-monochromatized MoK_α radiation. A total of 3697 symmetry-independent reflections was measured by the ω-scan technique at rates varying from 2 to 5° min^{-1}. The procedure followed in the data collection is described in Ref. (*2*). Only the 3037 reflections with intensities $I > 2\sigma$ (I) were used in the subsequent calculations which led to the structure determination. The net intensities were transformed into a set of structure amplitudes by the usual procedure using μ_l = 146.3 cm^{-1} for the absorption correction.

α-$Ba_9Fe_4S_{15}$

A black single crystal was selected from the 9BaS:4Fe:8S mixture reacted at 850°C and Weissenberg and Buerger photographs showed diffraction symmetry $4/m$ with systematic absences hkl, $h + k + l = 2n + 1$, $hk0$, $h = 2n + 1$, and $00l$, $l \neq 4n$; space group $I4_1/a$. A crystal measuring 0.12 × 0.11 × 0.10 mm was mounted on a quarter circle diffractometer and 47 reflections between 24 and 53° 2θ were measured with Mo radiation for input to a least-squares refinement for the parameters (*1*). The crystal data obtained at room temperature are shown in Table I. Three dimensional X-ray diffraction intensities to $\sin\theta/\lambda = 0.65$ were collected with the manual diffractometer using MoK_α radiation, a stationary crystal-stationary counter technique,

TABLE II

FINAL ATOMIC PARAMETERS AND THEIR STANDARD DEVIATIONS ($\times 10^4$) FOR β-$Ba_9Fe_4S_{15}$[a]

Atom	x	y	z	β_{11}	β_{22}	β_{33}	β_{12}	β_{13}	β_{23}
Ba(1)	3590(0)	5290(1)	1286(1)	3(0)	36(1)	24(0)	0(0)	0(0)	−2(1)
Ba(2)	140(0)	4860(1)	1805(1)	4(0)	45(1)	21(0)	−5(0)	−2(0)	3(1)
Ba(3)	1924(0)	5157(1)	3029(1)	5(0)	43(1)	37(1)	0(0)	4(0)	15(1)
Ba(4)	3573(0)	¾	4456(1)	5(0)	22(1)	25(1)		−3(0)	
Ba(5)	234(0)	¾	4607(1)	3(0)	21(1)	18(1)		−1(0)	
Ba(6)	2080(0)	¾	276(1)	1(0)	23(1)	21(1)		0(0)	
Fe(1)	3828(1)	¼	3206(2)	1(0)	32(3)	18(2)		1(1)	
Fe(2)	989(1)	¼	3700(2)	1(0)	22(3)	17(2)		0(1)	
Fe(3)	2755(1)	¼	813(2)	2(0)	32(3)	26(2)		0(1)	
Fe(4)	729(1)	¾	190(2)	1(0)	28(3)	19(2)		−1(1)	
S(1)	1523(2)	¾	4758(4)	2(1)	27(5)	28(3)		0(1)	
S(2)	4392(2)	¾	2216(4)	2(1)	32(5)	22(3)		1(1)	
S(3)	2978(2)	¼	2610(4)	2(1)	80(7)	22(3)		2(1)	
S(4)	4857(2)	¾	4923(4)	2(1)	42(5)	23(3)		1(1)	
S(5)	1133(2)	¼	1946(4)	6(1)	57(6)	17(3)		2(1)	
S(6)	1053(2)	¾	1884(4)	3(1)	44(5)	18(3)		−2(1)	
S(7)	1784(2)	¼	4547(4)	1(1)	28(5)	26(3)		−2(1)	
S(8)	2773(2)	¾	2452(4)	2(1)	29(5)	29(3)		−1(1)	
S(9)	4436(2)	¼	1960(4)	3(1)	47(5)	14(3)		3(1)	
S(10)	612(1)	4508(3)	4185(3)	4(0)	21(3)	21(2)	2(1)	−1(1)	−2(2)
S(11)	3953(1)	4376(3)	4272(3)	3(0)	24(3)	28(2)	1(1)	2(1)	1(2)
S(12)	2325(1)	4461(3)	497(3)	3(0)	23(3)	36(2)	1(1)	−2(1)	3(2)

[a] The temperature factor is $\exp[-(\beta_{11}h^2 + \beta_{22}k^2 + \beta_{33}l^2 + 2\beta_{12}hk + 2\beta_{13}hl + 2\beta_{23}kl)]$.

and balanced filters as was previously described (*1*). A total of 2021 independent reflections was measured and 1583 reflections were considered observed on the basis that peak counts exceeded background by 3σ. The measured intensities were transformed into a set of structure amplitudes by the usual procedure using $\mu_l = 146.3\ cm^{-1}$ for the absorption correction.

Structure Determination

β-$Ba_9Fe_4S_{15}$

The direct method employing the program MULTAN was used to calculate phases for the initial electron density map which yielded the Ba positions. Phases based on these positions and used in the calculation of the next Fourier map provided the locations of the other atoms. Full matrix least-squares refinement using the program NUCLS converged to $R = 0.064$ and $wR = 0.053$ for all 3697 reflections and $R = 0.049$ and $wR = 0.051$ for 3033 observed reflections. Values for the scattering factors for the neutral atoms, corrected for the real and complex parts of dispersion, were taken from Volume IV of the International Tables. The observed and calculated structure amplitudes are available.[1] The value of the isotropic extinction coefficient was 2.32×10^{-7}. The final difference electron density map showed random peaks and depressions with the highest values $\pm 4.5\ eÅ^{-3}$. Table II lists the atomic parameters.

[1] "See NAPS document no. 03234 for 27 pages of supplementary material. Order from NAPS c/o Microfiche Publications, P.O. Box 3513, Grand Central Station, New York, New York 10017. Remit in advance for each NAPS accession number. Institutions and Organizations may use purchase orders when ordering, however, there is a billing charge of $5.00 for this service. Make checks payable to Microfiche Publications." Photocopies are $6.75. Microfiche are $3.00 each. Outside the United States and Canada, postage is $3.00 for a photocopy and $1.00 for a fiche.

TABLE III

FINAL ATOMIC PARAMETERS AND THEIR STANDARD DEVIATIONS ($\times 10^4$) IN PARENTHESES FOR α-$Ba_9Fe_4S_{15}$[a]

Atom	x	y	z	β_{11}	β_{22}	β_{33}	β_{12}	β_{13}	β_{23}
Ba(1)	2281(1)	1441(1)	3406(0)	85(2)	32(1)	3(0)	15(1)	1(0)	−3(0)
Ba(2)	1294(1)	382(1)	7305(0)	56(1)	28(1)	2(0)	9(1)	−5(0)	−1(0)
Ba(3)	0	$\frac{1}{4}$	$\frac{5}{8}$	19(3)	19(3)	2(0)			
Fe	1344(2)	2075(2)	8302(1)	13(2)	27(3)	1(0)	5(2)	−1(1)	0(1)
S(1)	1003(4)	783(4)	5461(1)	23(4)	18(4)	2(0)	−6(4)	1(1)	0(1)
S(2)	1895(4)	1579(5)	8931(1)	19(4)	50(5)	2(0)	−11(4)	−1(1)	2(1)
S(3)	1764(5)	1924(5)	4349(1)	25(5)	23(4)	4(0)	2(4)	0(1)	2(1)
S(4)	0	$\frac{1}{4}$	$\frac{1}{8}$	39(16)	39(16)	26(2)			
S(5)[b]	3357(13)	2696(8)	2552(2)	432(27)	17(8)	6(1)	26(13)	−15(3)	2(2)
S(6)[c]	5753(23)	8046(23)	5461(5)	2(24)	−5(21)	0(2)	−12(20)	0(5)	−1(5)

[a] The temperature factor is $\exp[-(\beta_{11}h^2 + \beta_{22}k^2 + \beta_{33}l^2 + 2\beta_{12}hk + 2\beta_{13}hl + 2\beta_{23}kl)]$.
[b] Occupancy = 0.775(9).
[c] Occupancy = 0.154(10)

α-$Ba_9Fe_4S_{15}$

The direct method using MULTAN and an assumed composition $Ba_{30}Fe_{15}S_{54}$ generated 400 phases and the E-map based on them revealed four Ba and two Fe positions. An electron density map calculated from phased structure amplitudes obtained from these six atoms yielded the positions of the remaining atoms and also indicated that some sulfur atoms did not have full occupancy. A full matrix least-squares refinement was carried out with the program XFLS using only the atoms with full occupancy and anisotropic temperature factors, yielding $R = 0.087$ and $wR = 0.152$ for the observed reflections. An electron density difference map calculated with amplitudes from this refinement showed peaks which are labeled S(5) and S(6) in Table III. A final iteration in which all parameters were varied converged to $R = 0.0758$ and $wR = 0.0512$ for all reflections and $R = 0.0483$ and $wR = 0.0510$ for the observed reflections. The observed and calculated structure amplitudes are available.[1] The scattering factors for the neutral atoms, dispersion corrected for the real and complex part, were taken from Volume IV of the International Tables. The final difference electron density map showed random peaks and depressions with the highest values being ± 2.5 eÅ^{-3}. Table III lists the final atomic parameters.

Discussion of Structures

β-$Ba_9Fe_4S_{15}$

Table IV lists the bond distances and angles of interest. Figure 1 shows the projection of this structure together with the projections of the two other members of this series (*1*) to

TABLE IV

BOND DISTANCES AND ANGLES FOR β-$Ba_9Fe_4S_{15}$

Distances (Å)

Ba(1)–S(1)	3.309(1)	Ba(4)–S(2)	3.494(5)
S(2)	3.154(1)	S(4)	3.293(4)
S(3)	3.512(1)	S(5)	3.217(5)
S(7)	3.189(1)	S(8)	3.228(5)
S(8)	3.303(1)	2S(11)	3.155(3)
S(9)	3.525(1)	2S(12)	3.222(3)
S(10)	3.326(3)	Ba(5)–S(1)	3.256(4)
S(12)	3.435(3)	S(2)	3.124(4)
Ba(2)–S(2)	3.390(1)	S(9)	3.074(5)
S(4)	3.275(1)	2S(10)	3.253(3)
S(4)	3.413(1)	2S(10)	3.070(3)
S(5)	3.383(1)	Ba(6)–S(3)	3.356(5)
S(6)	3.426(1)	S(6)	3.284(5)
S(9)	3.272(1)	S(7)	3.010(4)
S(10)	3.239(3)	S(8)	3.248(5)
S(11)	3.317(3)	2S(11)	3.409(3)

TABLE IV—*Continued*

Ba(3)–S(1)	3.285(1)	2S(12)	2.992(3)
S(3)	3.719(1)	Fe(1)–S(3)	2.273(5)
S(5)	3.510(1)	S(9)	2.193(5)
S(6)	3.456(1)	2S(11)	2.267(3)
S(7)	3.204(1)	Fe(2)–S(5)	2.237(5)
S(8)	3.187(1)	S(7)	2.268(5)
S(10)	3.665(3)	2S(10)	2.234(3)
S(12)	3.409(3)	Fe(3)–S(1)	2.253(5)
S(12)	3.653(3)	S(3)	2.330(6)
		2S(12)	2.209(3)
Fe(4)–S(4)	2.203(5)	S(3)–S(7)	3.872(6)
S(6)	2.282(5)	S(9)	3.767(6)
2S(11)	2.285(3)	S(11)	3.697(1)
S(1)–S(6)	3.801(7)	S(12)	3.650(3)
S(10)	3.746(3)	S(4)–S(11)	3.854(3)
S(3)	3.804(7)	S(5)	3.567(7)
S(9)	3.677(6)	S(6)	3.777(6)
S(12)	3.584(3)	S(11)	3.641(3)
S(2)–S(4)	3.603(6)	S(5)–S(7)	3.658(7)
S(8)	4.096(6)	S(10)	3.657(3)
S(11)	4.111(3)	S(12)	3.986(3)
S(10)	4.271(3)	S(6)–S(11)	3.747(3)
		F(1)–Fe(4)	2.734(4)

Angles (degrees)

S(11)–Fe(1)–S(9)	109.0(1)
S(11)–Fe(1)–S(3)	109.1(1)
S(11)–Fe(1)–S(11)	105.2(2)
S(9)–Fe(1)–S(3)	115.1(2)
S(10)–Fe(2)–S(7)	104.3(1)
S(10)–Fe(2)–S(5)	109.8(1)
S(10)–Fe(2)–S(10)	119.3(2)
S(7)–Fe(2)–S(5)	108.6(2)
S(12)–Fe(3)–S(3)	107.0(1)
S(12)–Fe(3)–S(1)	106.9(1)
S(12)–Fe(3)–S(12)	117.0(2)
S(3)–Fe(3)–S(1)	112.2(2)
S(6)–Fe(4)–S(11)	110.3(1)
S(6)–Fe(4)–S(4)	114.7(2)
S(11)–Fe(4)–S(4)	108.5(1)
S(11)–Fe(4)–S(11)	104.0(1)

accentuate the similarities and also emphasize the differences. Fe is in tetrahedral coordination to S, while the coordination polyhedron around Ba is either a capped trigonal prism or a bisdisphenoid. One isolated trinuclear tetrahedral unit in which the central tetrahedron shares one edge and one corner, one binuclear unit in which the two tetrahedra share an edge, and one isolated tetrahedron are present in the asymmetric unit.

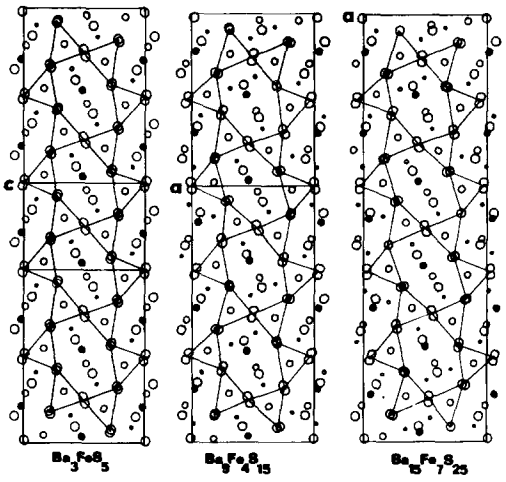

FIG. 1. Projection along the y axis of three compounds in $Ba_3Fe_{1+x}S_5$ showing 1, $1\frac{2}{3}$, and 5 unit cells. The vertical axes are labeled. The large circles are S, the smaller circles are Ba, and the smallest Fe. S at the corners of the prism are at $y = \frac{1}{4}, \frac{3}{4}$; Ba within the prisms are at $y \approx 0, \frac{1}{2}$. Within the hexagonal rings Ba and Fe at $y = \frac{3}{4}$ are indicated by filled circles, while those at $y = \frac{1}{4}$ are open, and the S are at $y \approx 0, \frac{1}{2}$.

The Ba–S framework of interlinked distorted trigonal prisms is common to the structures. The fundamental unit cell of dimensions 12.4 × 9.5 × 8.5 Å contains two pseudohexagonal rings formed by edge sharing of trigonal prisms and they are stacked along the 9.5-Å axis by sharing the triangular prismatic faces. The framework content in the fundamental unit cell is thus Ba_8S_{12}. Within each ring are two additional Ba at $y = \frac{1}{4}$ and $\frac{3}{4}$, and 4 S at $y \approx 0, \frac{1}{2}$, so that the total unit cell content is $Ba_{12}S_{20}$. There are six tetrahedral sites (not indicated in Fig. 1) within a ring or twelve per unit cell. Three sites, however, are in a trinuclear unit in which the central tetrahedron shares faces with the other two and these three sites cannot be filled simultaneously. Filling only the site in the central tetrahedron gives rise to 2 Fe per ring or 4 Fe in the fundamental unit cell for a cell content of $Ba_{12}Fe_8S_{20}$, i.e. Ba_3FeS_5, which constitutes one end member of the series. If the two outside tetrahedra of the trinuclear units are occupied, the fundamental unit cell has the composition $Ba_{12}Fe_8S_{20}$ or $Ba_3Fe_2S_5$, the other end member of the series which has not yet

been synthesized. It is noteworthy that the formal oxidation state of Fe changes from 4+ to 2+ for the two end members. The high oxidation state compound is only stable at high pressure (*1*).

In the compound $Ba_{15}Fe_7S_{25}$, or $Ba_3Fe_{1.4}S_5$, one ring has 4 Fe, two rings have 3 Fe, and two rings have 2 Fe, the sequence being 2–3–4–3–2, so that the periodic repeat unit is approximately five times the fundamental length of 8.5 Å. The compound $Ba_9Fe_4S_{15}$, or $Ba_3Fe_{1.333}S_5$, has three rings per periodic repeat in which the tetrahedral occupancies are 3–2–3 and the unit cell parameter is close to $3 \times 8.5 = 25.5$ Å.

It is possible to predict structures in this series subject to the constraints that the iron valence be limited to 2+ and 3+ and that the space group remain *Pnma*. Thus the general formula can be written as $(Ba_3S_5)_{4p}Fe_{4q}$, p and q integers, where p is the number of rings along the axis, $4p$ is the negative charge of the framework, and $2q$ is the tetrahedral occupancy of the p rings.

Table V lists all possible compounds up to seven rings, i.e., a lattice parameter of about 60 Å. If the constraint of 3+ as the maximum iron valence is removed then more possibilities arise but these can probably be realized only at high pressures as in the Ba_3FeS_5 end member.

TABLE V

POSSIBLE COMPOSITIONS IN THE SERIES $Ba_3Fe_{1+x}S_5$ OR $(Ba_3S_5)_{4p}Fe_{4q}$ TO $p = 7$

p	q	Fe Valence [ave]	x
1	1	4[a]	0[b]
1	2	2	1.000
2	3	2(+3),1(+2)[2.67]	0.500
3	4	3	0.333[b]
3	5	2(+3),3(+2)[2.4]	0.667
4	7	2(+3),5(+2)[2.286]	0.750
5	7	6(+3),1(+2)[2.857]	0.400[b]
5	8	4(+3),4(+2)[2.5]	0.600
5	9	2(+3),7(+2)[2.222]	0.800
6	11	2(+3),9(+2)[2.182]	0.833
7	10	8(+3),2(+2)[2.8]	0.429
7	11	6(+3),5(+2)[2.545]	0.571
7	12	4(+3),8(+2)[2.333]	0.714
7	13	2(+3),11(+2)[2.154]	0.857

[a] High-pressure phase.

[b] Synthesized phase.

Each composition gives rise to a definite compound, i.e., x has a fixed value, so that this series is another example which fits the definition of "infinitely adaptive" (*3*). This is the second instance of such a series in the Ba–Fe–S system (*4*).

α-Ba₉Fe₄S₁₅

The structural scheme of this compound is best described in terms of overlapping sections along the c axis. The sections are chosen on the basis of Ba ions with nearly the same z parameters, so that Ba(1) and Ba(3) define one section and Ba(2) defines the other one. Within the section $0.24 \leqslant z \leqslant 0.46$, Fig. 2, Ba(1) is coordinated by three S(2), S(1), S(4), and S(5), which form a fairly regular trigonal prism with the axis parallel to [120]. Ba(3) is on a $\bar{4}$ axis and is coordinated by four S(2) which form a flat bisphenoid and four S(1) which form an elongated bisphenoid and they are rotated by about 30° to each other so that the polyhedron is a distorted bisdisphenoid. These are

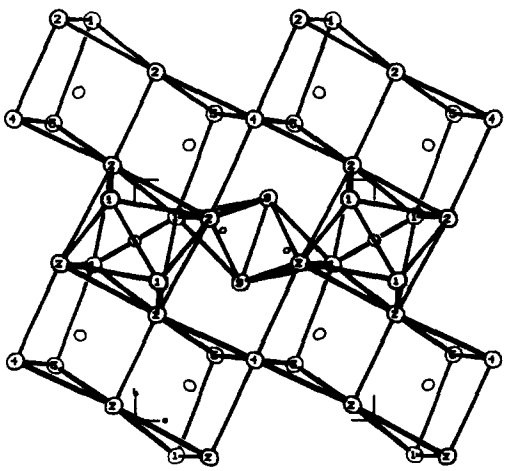

FIG. 2. The section $0.24 \leqslant z \leqslant 0.46$ for α-$Ba_9Fe_4S_{15}$ showing the coordination around Ba(1) and Ba(3). Circles with numbers are the different S, the smaller circles are Ba, and the smallest Fe.

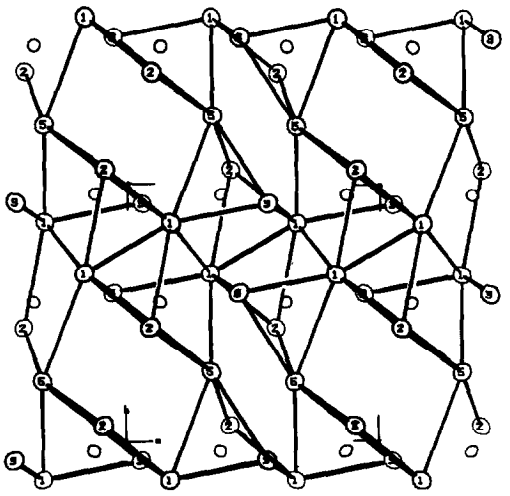

FIG. 3. The section $0.14 \leqslant z \leqslant 0.36$ for α-$Ba_9Fe_4S_{15}$ showing the Ba(2) layer.

the same types of coordination polyhedra found in the β phase. The Ba(1) trigonal prisms share one edge formed by S(2) and the sets of two prisms connect by corner sharing of S(4) into infinite zigzag chains parallel to [100]. The two parallel chains are bridged by Ba(3) polyhedra. Two of the triangular faces of each bisdisphenoid are also part of a trigonal prism from each chain. The Ba(3) polyhedra are isolated, i.e., they do not share faces, edges, or corners with other Ba(3) polyhedra. Thus an enclosed space is created by four Ba(1) prisms, two from each chain which share corners at S(4) and by two Ba(3) polyhedra which span them. Within this space are located the isolated pairs of edge sharing FeS_4 tetrahedra.

The section defined by Ba(2), $0.14 \leqslant z \leqslant 0.36$, is shown in Fig. 3. The cation is in a distorted trigonal prism formed by three S(1), S(2), S(3), and S(5). Rows of trigonal prisms exist parallel to [$\bar{2}$30]. The units within a row consist of two edge-sharing prisms with a dihedral angle of 60° (59.8°) between two triangular faces. If the row in Fig. 3 with the prism units oriented so that the triangular faces are directed upward is labeled A, then the adjacent row B, with the trapezoidal faces showing, is produced by a 180° rotation of A around [$\bar{2}$30] as an axis. A unit from A shares an edge with a unit from B; the shared edge being the height of the prism. The same unit of A also shares a corner with the next unit of B. The triangular faces of the two prisms formed by S(1)–S(1)–S(2) are also faces of the bisdisphenoid. The edges S(5)–S(2), S(1)–S(2), and S(5)–S(1) are common with those of the Ba(1) prism shown in Fig. 2. All Ba ions are in eight-fold coordination because the corners of prisms also cap two of the rectangular faces of neighboring prisms, e.g., S(5) caps the faces S(5)–S(3)–S(1)–S(2) of a Ba(2) prism and S(5)–S(4)–S(2)–S(1) of a Ba(1) prism, and S(3) caps the faces S(2)–S(5)–S(1)–S(1) of a Ba(2) prism and S(2)–S(5)–S(1)–S(2) of a Ba(1) prism. The S(3)–S(3) distance is the shared edge between the binuclear tetrahedral unit in the level $0.24 \leqslant z \leqslant 0.46$.

The level $0.29 \leqslant z \leqslant 0.51$ is identical to that of $0.24 \leqslant z \leqslant 0.46$ and is produced by rotating

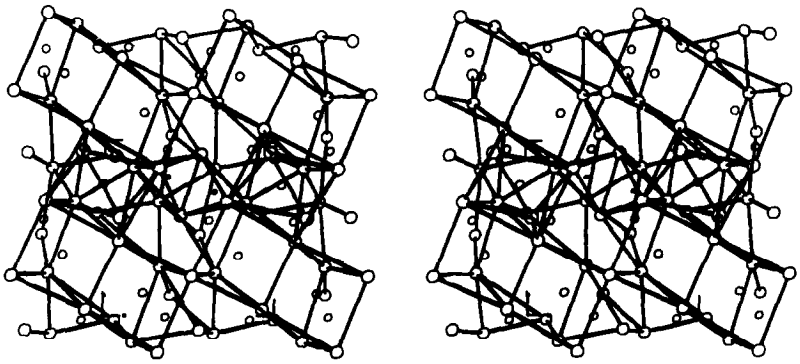

FIG. 4. Stereoscopic view of the Ba(2) layer fused to the Ba(1)–Ba(3) layer of α-$Ba_9Fe_4S_{15}$.

the lower section around the $\bar{4}$ axis passing through 0, $\frac{1}{4}$, $\frac{3}{8}$, the Ba(3) position. This section articulates again with a Ba(2) section appropriately positioned at the level $0.39 \leqslant z \leqslant 0.61$. The unit Ba(2)–[Ba(3), Ba(1)]–Ba(2) is then repeated along the c axis by the space group symmetry to complete the structure. Fig. 4 is a stereoscopic view of a Ba(2) level fused to a [Ba(1), Ba(3)] level.

The bond distances in Table VI show several unrealistic values. We propose that in the case of S(5) only one of two mutually exclusive sets of eight equivalent positions is possible in the structure. Either S(5) at 0.3357, 0.2696, 0.2552, and its equivalent positions produced by the operation $I\bar{4}$ are present, or S(5) at 0.1643, 0.2304, 0.2448, and its symmetry related positions by $I\bar{4}$ exist. The first set of positions of S(5) produces a more symmetrical Ba(2) prism than the second set and perhaps the latter never occurs in the structure. Other models can be selected in which S_2 units are present, e.g., formed by S(5)–S(6). The refinement converges to some averaged positional parameters for S(5) and S(6) and with small shifts in the parameters bond distances for S_2 consistent with expected values can be realized. The data from the "single" crystal do not permit a decision to be made among the different possibilities. The various structures, differing only in the S(5) and S(6) locations, may well be present within one crystal on the level of unit cell dimensions.

TABLE VI

BOND DISTANCES AND ANGLES FOR α-$Ba_9Fe_4S_{15}$

Distances (Å)

Ba(1)–S(1)	3.260(4)	Fe–Fe	2.718(3)
S(2)	3.183(5)	S(1)–S(1)	3.832(6)
S(2)	3.516(4)	S(1)	4.007(5)
S(2)	3.235(4)	S(2)	3.588(5)
S(3)	3.309(4)	S(2)	3.858(6)
S(4)	3.050(1)	S(3)	4.039(5)
S(5)	3.441(8)	S(3)	3.786(6)
S(5)	3.329(8)	S(3)	3.847(6)
S(6)	3.124(21)	S(5)	4.066(12)
S(6)	3.514(21)	S(2)–S(2)	4.059(6)
Ba(2)–S(1)	3.148(4)	S(3)	3.887(6)
S(1)	3.225(4)	S(3)	3.677(5)
S(1)	3.171(4)	S(3)	3.935(6)
S(2)	3.164(4)	S(3)–S(3)	3.579(6)
S(3)	3.413(4)	S(4)	3.776(4)
S(3)	3.434(4)	S(5)	3.729(11)
S(5)	3.291(8)	S(6)	2.480(22)
S(5)	3.102(7)	S(4)–S(6)	2.856(18)
S(6)	3.780(22)	S(5)–S(5)	1.694(17)
S(6)	3.523(20)	S(5)	3.226(18)
Ba(3)–4S(1)	3.315(4)	S(6)	1.845(21)
4S(2)	3.182(4)	S(6)	2.709(23)
Fe–S(1)	2.272(4)	S(6)	3.336(23)
S(2)	2.276(4)	S(6)–S(6)	1.795(31)
S(3)	2.317(5)		
S(3)	2.296(5)		

Angles (degrees)

S(3)–Fe–S(3)	101.8(2)
S(3)–Fe–S(1)	112.0(2)
S(3)–Fe–S(2)	118.8(2)
S(3)–Fe–S(1)	113.9(2)
S(3)–Fe–S(2)	106.4(2)
S(1)–Fe–S(2)	104.2(2)

Another ambiguity is present in this structure. Difference electron density maps definitely indicate the presence of electron density near the S(5) position, and placing atom S(6) into the indicated location and subsequent least-squares refinement yielded the parameters shown in Table III. The 16-fold S(6) positions give rise to bond distances shown in Table VI and again some of them are not realistic.

Pairs of S(6) atoms 1.8 Å apart lie within the spaces such as outlined by S(1)–S(5)–S(3)–S(1)–S(5)–S(2)–S(1) in Fig. 3. If the assumption is made that only half the rings are occupied at a given time by S(6) units, then a selection can be made whereby unrealistic distances with a set of S(5) atoms are eliminated. However, short distances still occur with S(3) and S(4). The low-occupancy factor combined with the large uncertainties in the positions of S(6) make a meaningful interpretation of bond distances impossible. Sterically there is space available for a S atom within such a ring and probably only one S(6) per ring is present, or eight atoms in the unit

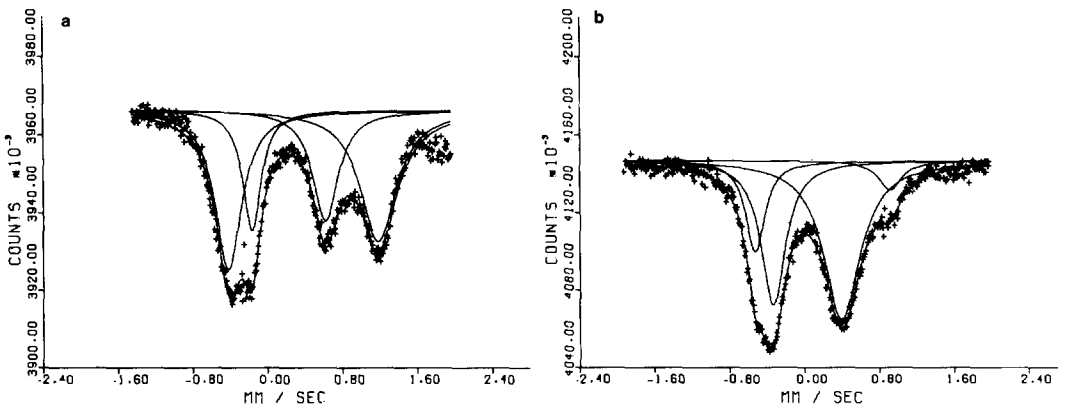

FIG. 5. Observed room temperature Mössbauer spectra of (a) α, (b) β-$Ba_9Fe_4S_{15}$. The calculated spectrum is fitted by least squares.

cell and at locations which do not create impossible distances, which result only because the X-ray structure determination sees averages over many unit cells.

There is no structural relationship between the α and β forms except that trigonal prisms and bisdisphenoids occur in both.

The Mössbauer diagrams for the two phases are shown in Figs. 5a and b. Two sets of quadrupole split lines were fit to the spectra, which yielded isomer shift values for the α phase of 0.39 and 0.26 mm/sec and 0.37 and 0.21 mm/sec for the β phase. We have previously related the isomer shift with the oxidation state of Fe(5) and the values for the β phase indicate that some electron delocalization within the binuclear unit is present. The spectrum for the α phase, which has only one crystallographic iron, must reflect the presence in the structure of various twins. Thus the presence of S_2 would decrease the formal valence of iron and give rise to the observed values of the isomer shifts intermediate between 2+ and 3+. This has been observed to be the case when the Fe–Fe distance is about 2.6 to 2.7 Å. The Fe^{3+} indicated by the 0.21 mm/sec value for the β phase should be Fe in the isolated tetrahedron and in the tetrahedron that shares a corner in the trinuclear unit (*1*).

Acknowledgments

The authors gratefully acknowledge the research support provided by the Robert A. Welch Foundation, Houston, Texas, and by the National Science Foundation.

References

1. J. T. LEMLEY, J. M. JENKS, J. T. HOGGINS, Z. ELIEZER, AND H. STEINFINK, *J. Solid State Chem.* **16**, 117 (1976).
2. P. E. RILEY AND R. E. DAVIS, *Inorg. Chem.* **14**, 2507 (1975).
3. J. S. ANDERSON, *J. Chem. Soc. Dalton Trans.*, 1107 (1973).
4. J. T. HOGGINS AND H. STEINFINK, *Acta Crystallogr. B* **33**, 673 (1977).
5. J. T. HOGGINS AND H. STEINFINK, *Inorg. Chem.* **15**, 1682 (1976).